

## Article

# Evaluation of Fume Suppression, Viscosity-Retarding, and Rheological Properties of Eco-Friendly High-Viscosity Modified Asphalt

Weidong Ning, Guoqiang Sun , Kexin Qiu, Xulai Jiang, Chunze Wang and Ruiqi Zhao

Beijing Key Laboratory of Traffic Engineering, Beijing University of Technology, Beijing 100124, China

\* Correspondence: gqsun@bjut.edu.cn

**Abstract:** In order to address the issues of high viscosity and excessive fume exhaust associated with high-viscosity modified asphalt (HVMA), the objective of this study was to develop an eco-friendly HVMA by incorporating fume suppressants and viscosity-retarding agents (VRAs). To begin with, desulfurization rubber powder (DRP) was utilized as a modifier, and fume suppressants, including activated carbon, a chemical reaction fume suppressant, and a composite fume suppressant combining activated carbon and chemical reaction fume suppressant were added to the HVMA separately. The fume suppression effect and odor level were observed to determine the optimal fume suppressant composition for this study. Based on these observations, an area integration method was proposed, utilizing rotational viscosity testing and temperature sweeping experiments, evaluating the viscosity-retarding effect and mixing temperature when different amounts of Sasobit VRA, Evotherm3G VRA, and a composite VRA of Sasobit and Evotherm3G were added to the HVMA. This approach aimed to identify the eco-friendly HVMA with the most effective fume suppression and viscosity-retarding abilities. Furthermore, the morphology and rheological properties of the eco-friendly HVMA were examined through fluorescence microscopy, zero shear viscosity test, multiple stress creep recovery analysis, liner amplitude sweep test, and frequency sweep test. The results demonstrated that the HVMA formulation consisting of 15% DRP and 1% composite fume suppressant exhibited a satisfactory fume suppression effect and odor level. Based on this, the HVMA formulation containing 0.6% Evotherm3G and 3% Sasobit VRAs displayed the best viscosity-retarding effect while reducing the mixing temperature. Moreover, when compared to common HVMA, the eco-friendly HVMA exhibited excellent high-temperature resistance, successfully accomplishing the dual objectives of ecological friendliness and superior performance.

**Keywords:** eco-friendly high-viscosity modified asphalt; viscosity retarding; fume suppression; rheological properties



**Citation:** Ning, W.; Sun, G.; Qiu, K.; Jiang, X.; Wang, C.; Zhao, R. Evaluation of Fume Suppression, Viscosity-Retarding, and Rheological Properties of Eco-Friendly High-Viscosity Modified Asphalt. *Coatings* **2023**, *13*, 1497. <https://doi.org/10.3390/coatings13091497>

Academic Editors: Hadj Benkreira and Valeria Vignali

Received: 12 July 2023

Revised: 19 August 2023

Accepted: 23 August 2023

Published: 24 August 2023



**Copyright:** © 2023 by the authors. Licensee MDPI, Basel, Switzerland. This article is an open access article distributed under the terms and conditions of the Creative Commons Attribution (CC BY) license (<https://creativecommons.org/licenses/by/4.0/>).

## 1. Introduction

During the process of urban construction, high-viscosity modified asphalt (HVMA) had attracted significant attention from researchers due to its remarkable performance in both high and low temperatures as well as its superior durability. However, the high mixing temperature of HVMA led to the emission of a considerable amount of asphalt smoke during the production process, particularly for CRMA. The production process of CRMA often generated more asphalt smoke compared to ordinary HVMA. This not only posed a serious threat to human health but also resulted in severe pollution to the surrounding environment. Consequently, these issues greatly impeded the extensive adoption and application of HVMA in pavement engineering [1–3].

Asphalt fume predominantly consisted of volatile organic compounds (VOCs), polycyclic aromatic hydrocarbons (PAHs), sulfur oxides, and nitrogen oxides. VOCs, in terms of content and type, represented the majority, with alkanes, olefins, alkynes, benzene

series, and hydrocarbon derivatives (such as aldehydes and ketones) being the main constituents [4]. Inhalation of these compounds could lead to respiratory difficulties, organ damage, and even cancer [5]. PAHs, which were a distinct category of VOCs, were typically considered to be separate components of asphalt fume. They contained highly carcinogenic substances like acyclic naphthalene, fluoroanthracene, fluorene, naphthalene, benzene, and pyrene, posing significant threats to human health [6]. Therefore, reducing the release of asphalt fumes and energy consumption of HVMA have nowadays become a prominent research area in road engineering [7].

Fundamentally, variations in production temperature played a crucial role in causing changes in asphalt fume emissions. Elevated temperatures caused the macromolecular organic compounds in asphalt materials to undergo thermolysis, resulting in the formation of smaller molecules. With increasing temperatures, the intensity of Brownian motion was heightened, enabling the escape of small molecules from the organic interface. By disrupting the Van der Waals forces between asphalt molecules, these small molecules subsequently combined with gases, steam, and aerosols external to the organic interface, forming asphalt fumes [7,8]. However, it is important to note that there were significant differences in the physical and chemical properties between waste rubber and asphalt. These differences resulted in the poor stability and compatibility of asphalt when waste rubber was used as an additive. Specifically, at high temperatures, the components of waste rubber were more susceptible to separation, which led to the release of sulfur-containing smoke and volatile organic compounds [2,9].

Currently, fume detection methods primarily consist of indoor and on-site detection techniques, including gravimetric, UV-Vis, and sampling detection techniques [10,11]. The gravimetric method only permits the measurement of asphalt fume mixture concentration, whereas the UV visible method allows for the determination of both the concentration of asphalt fume mixtures and the content of individual polycyclic aromatic hydrocarbons [1,11,12]. Sampling detection technology enables the measurement of the composition and concentration of polycyclic aromatic hydrocarbons (PAHs) in asphalt smoke. Gas chromatography–mass spectrometry (GC-MS) is presently one of the principal methods employed for quantitatively characterizing and qualitatively analyzing different components of asphalt fume [13–15]. Tang et al., conducted an analysis of fume emissions from the production process of CRMA using activated carbon adsorption tubes. The collected samples were further analyzed through GC-MS. The researchers discovered that CRMA contained nine new compounds that were not present in pure asphalt [3]. Moreover, the presence of internal sulfur bonds in CRMA led to the release of more volatile sulfur compounds (VSCs). These VSCs included hydrogen sulfide, benzothiazole, 3-methylthiophene, 2-methylthiophene, and others [2,16]. It is worth noting that these compounds possess strong carcinogenic properties, posing a significant threat to human health [2,4].

In order to mitigate asphalt fume pollution, researchers typically added different types of fume suppressants to HVMA [17–19]. Lv et al., developed a fume suppressant named UiO-66 and evaluated its effectiveness in reducing fume production. Its impact on the concentration of class 1 carcinogens in CRMA was assessed through GC-MS analysis. The results showed that the addition of UiO-66 resulted in the reduction in class 1 carcinogens concentration in CRMA by 70% [18]. Li et al., aimed to address the root cause of malodorous gases in rubber-modified asphalt and devised a composite modifier using desulfurized rubber powder (DRP) and styrene–butadiene–styrene (SBS). Through desulfurization, the number of disulfide bonds in the rubber was reduced, thereby minimizing the release of malodorous gases. The study determined that the optimal proportions were 15% DRP and 4% SBS. Remarkably, the performance of the modified asphalt with this composite modifier surpassed that of the single-component SBS, resulting in a reduction of over 40% in SO<sub>2</sub> emissions, as well as reductions exceeding 50% in nitrogen dioxide (NO<sub>2</sub>) and nitrogen oxide (NO<sub>x</sub>) emissions [19]. This provided a new approach for this study. However, it was worth noting that during this period, most studies only added traditional smoke inhibitors

during the process and did not develop efficient target smoke suppressants for asphalt and asphalt fume components, which should be the direction of future research.

Nowadays, people often reduce the viscosity of HVMA by adding warm mixing agents, thereby indirectly reducing the energy consumption of HVMA [20]. Various warm mix additives such as organic waxes, surfactants, and foaming techniques have been utilized [21–24]. In terms of organic waxes, Jamshidi et al., conducted a review on the rheological properties and performance of asphalt-containing Sasobit, along with its potential for energy-saving and reduction in greenhouse gas emissions. They found that the incorporation of Sasobit resulted in a 17.9% reduction in natural gas consumption and a 10% reduction in the use of recycled oil as industrial fuel [21]. Furthermore, Wan et al., investigated the modification of asphalt using a surfactant called Evotherm, along with aluminum hydroxide (ATH). Their findings indicated that the modified asphalt exhibited improved thermal stability [22]. Additionally, researchers such as Valdes-Vidal et al., had utilized natural zeolite in the preparation of WMA. Their study demonstrated that the incorporation of recycled pavement allowed for lower-temperature mixing and construction, with promising road performance [23]. However, despite the benefits they offer, warm mix additives still have some drawbacks as they can potentially negatively impact the performance of asphalt while lowering the mixing temperature. Therefore, further research is needed to investigate the effects of additive types and dosages on the performance of WMA [24].

To enhance the performance of WMA, researchers have proposed a technology called warm-mix-based viscosity-retarding asphalt (WM-VRA) [25]. This innovative approach reduces the mixing temperature by implementing higher-temperature viscosity-retarding techniques, extends the working time through medium-temperature viscosity-retarding methods, and improves the service viscosity within lower temperature ranges. By achieving both viscosity-retarding and energy-saving goals, WM-VRA ensures the performance of HVMA. Furthermore, this paper introduces an area integration method for viscosity–temperature curves. By comparing the integration areas of viscosity–temperature curves between various types of WM-VRA and traditional HVMA at different temperatures, we can evaluate the viscosity-retarding effect of WM-VRA. This research provides a foundation for selecting HVMA that could maintain their performance while also being energy-saving and viscosity-retarding.

This study aims to address the limitations of traditional fume suppressants on modified asphalt components and the decreased performance of traditional WMA. To achieve this, an eco-friendly HVMA was developed through the optimization of fume suppressants and viscosity-retarding agents (VRAs), and the rheological properties of this eco-friendly asphalt were assessed against standards. The study focused on several key factors. First, indoor fume evaluations and odor level were conducted to compare the fume suppression effects of activated carbon, chemical reaction fume suppressants, and composite fume suppressants on DRP-modified HVMA and rubber-modified HVMA. The optimal combination of fume suppressants was then identified. Building on these findings, different amounts of Sasobit VRA, Evotherm3G VRA, and a composite VRA of Sasobit and Evotherm3G were added to screen for the most effective eco-friendly HVMA in terms of fume suppression and viscosity-retarding effects. The mixing temperature and viscosity-retarding properties of the HVMA were evaluated using rotating viscosity, temperature sweep, and viscosity–temperature line integral area tests. Finally, the morphological characteristics and rheological properties of the eco-friendly HVMA were confirmed through fluorescence microscopy and dynamic shear rheological tests, demonstrating the feasibility of its performance. This study presented a research and development framework for eco-friendly HVMA, which aims to reduce asphalt fume emissions and decrease energy consumption during asphalt pavement construction, thereby promoting a green and low-carbon approach to asphalt pavement development.

## 2. Materials and Methods

### 2.1. Raw Materials

This study utilized Shell 70# asphalt as the base matrix asphalt. Based on a series of preliminary experiments and the relevant literature, the following additives were selected to prepare the high-viscosity modified asphalt (HVMA): 0.15% sulfur, 4% styrene–butadiene–styrene (SBS), 0.75% polyphosphoric acid (PPA), 0.5% antioxidant, and 15% desulfurization rubber powder (DRP) [17,19]. To determine the most effective fume suppressant, 1% activated carbon, 1% chemical reaction fume suppressant, and 1% composite fume suppressant were added to the HVMA separately. Comparative samples included rubber-powder HVMA with the same components, blank rubber-powder HVMA, and blank DRP-modified asphalt. Indoor fume and odor-level evaluations were conducted to assess the feasibility of reducing fume emissions using DRP and to identify the optimal fume suppressant formulation (as shown in Figure 1).

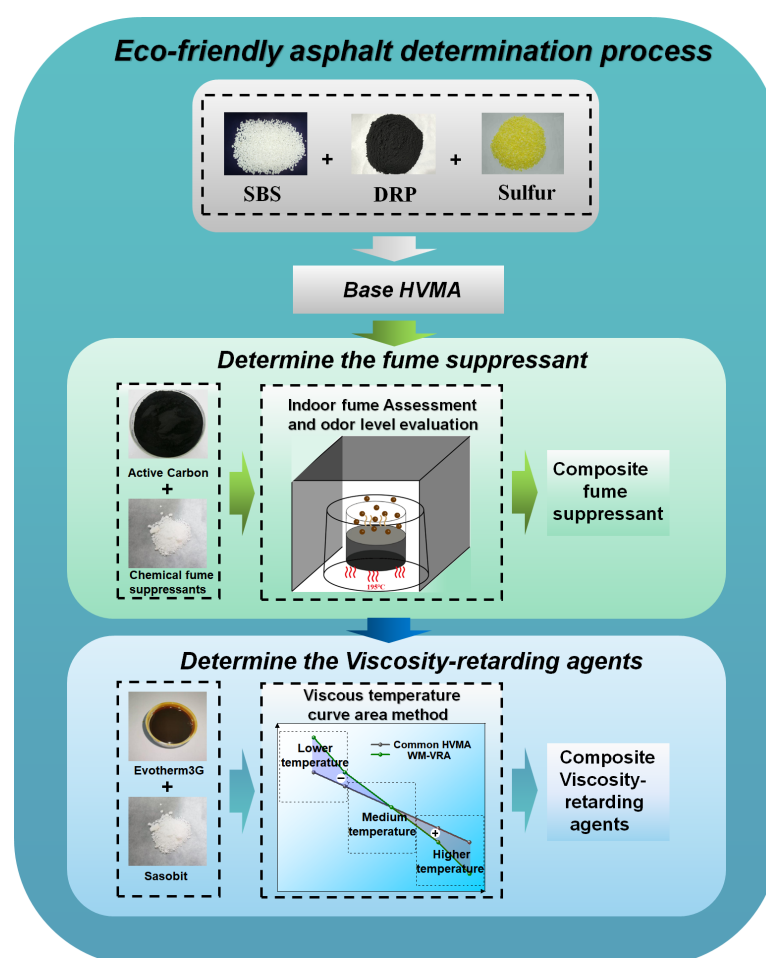


**Figure 1.** Eco-friendly asphalt determination process.

Subsequently, in the previously optimized fume-suppressing HVMA, different percentages of Sasobit were incorporated, namely 2% Sasobit, 3% Sasobit, 0.5% Sasobit, 0.6% Sasobit, 0.5% Evotherm3G + 2% Sasobit, and 0.6% Evotherm3G + 3% Sasobit [19,20]. Through FM analysis, rotational viscosity testing, and rheological performance testing, eco-friendly HVMA with a remarkable viscosity-retarding effect and exceptional rheological properties was chosen.

In this experiment, the chemical reaction fume suppressant utilized a mixture comprising 75% zinc ricinoleate, 20% sulfurization promoter, 2.5% magnesium sulfate, and 2.5% silane coupling agent. The sulfurization promoter component consisted of stearic acid and zinc oxide. To obtain the composite fume suppressant, the chemical fume suppressant

was combined with activated carbon in a 1:1 ratio. The silane coupling agent was prepared by blending KH550 and KH560 in a 1:1 ratio.

## 2.2. Preparation of the Modified Asphalt Samples

The preparation process of eco-friendly HVMA was as follows:

- (1) The base asphalt was heated to a temperature of 180~190 °C, SBS was then added and stirred for 10 min, followed by shearing for 15 min at a speed of 1000~3000 r/min. DRP was added in batches, stirred for 10 min, and sheared for 60 min at a speed of 4000~6000 r/min.
- (2) PPA and sulfur were added and sheared for 10 min at a speed of 4000~6000 r/min. Viscosity-retarding agents (VRAs) and antioxidants were then added and sheared for 10 min at a speed of 3000~5000 r/min. Finally, fume suppressant was added and sheared for 10 min at a speed of 4000~6000 r/min.
- (3) The temperature was lowered to a range of 170~180 °C, and a four-blade mixer operating at a speed of 600 r/min was used for low-speed stirring for 30 min to eliminate foaming. Subsequently, the mixture was taken out and placed in an oven at 170~180 °C for 30 min to undergo swelling and development.
- (4) Once the product was inspected and deemed qualified, it was certified as an eco-friendly HVMA and stored for insulation.

## 2.3. Experimental

### 2.3.1. Fluorescence Microscopy (FM) Observation

The FM sample of HVMA was prepared through the hot casting method. The FM micrographs were captured at room temperature using the Olympus Fluorescence microscope system, and a series of images with magnifications of 10 and 20 were obtained. This method was used to observe the crosslinking of HVMA and the distribution of modifiers.

### 2.3.2. Indoor Fume Assessment

In this study, the fume suppression effect was evaluated by observing the fume release of different fume-reducing asphalt materials. Firstly, in a fume hood, the 10 g of asphalt was heated to 185 °C for ten minutes. A video recording was then started with a duration of 1 min to monitor the fume release of different HVMA. Finally, images of HVMA fume release at 30 s were collected for comparative analysis.

### 2.3.3. Odor-Level Evaluation

To assess the intensity of unpleasant odor emitted by high viscosity asphalt, this study employed the Japan Odor Discomfort Scale (JODS) developed by the Ministry of Land, Infrastructure, Transport, and Tourism (MLIT) in Japan. JODS categorized odor levels on a scale ranging from 0 to 5, denoting the absence of discomfort (level 0) to the maximum extent of discomfort (level 5) (Table 1).

**Table 1.** Japanese odor-level evaluation.

| Strength | Grade   |
|----------|---|
| 0        | No odor   |
| 1        | Can barely feel the odor                        |
| 2        | The odor is weak but can distinguish properties |
| 3        | Easy to feel the odor                           |
| 4        | Strong odor                                     |
| 5        | An unbearable strong odor                       |

The experiment recruited 10 participants, including 5 males and 5 females, aged between 25 and 50 years old. They were provided with standardized guidelines for scoring the odorous experience. During the evaluation process, participants described and

evaluated the odor based on their personal perception and experiences, taking into account factors such as the intensity, discomfort level, color, and duration of the odor stimulus.

The scores provided by the participants, which ranged from 0 to 5, reflected their individual perceptions of the intensity and level of discomfort associated with the odor. Statistical analysis was employed to summarize and report the evaluation results. The interpretation of these results allowed for a comprehensive description and understanding of the odor levels, with higher scores indicating heightened levels of odor perception and discomfort.

#### 2.3.4. Viscosity Test Performed by Rotational Viscometer

In this study, the rotational viscosity test was conducted using the Brookfield viscometer method [26]. The test was mainly performed using a rotational viscometer to measure the apparent viscosity of road asphalt within the temperature range above 155 °C. This measurement was used to determine the construction temperature of various asphalt mixtures and provides a data basis for viscosity-retarding evaluation. The test results might be influenced by external factors, so it was common practice to take the average of three readings as the result during the experiment.

#### 2.3.5. Temperature Sweep (TS) Test

In order to monitor the rheological properties of asphalt as it ages over a wide temperature range, temperature scanning tests were conducted from low temperature to high temperature (30 °C to 100 °C, intervals of 10 °C) at a constant frequency of 10 Hz and a strain of 1%. Throughout the process, a plate with a geometry shape of 8 mm and a gap of 1 mm was used for oscillation testing. The complex shear modulus ( $G^*$ ) and phase angle ( $\delta$ ) at different temperatures were obtained. Three repeated averages were used, and the coefficient of variation was kept within 5%. This method was used to measure the complex viscosity of HVMA from 30 °C to 100 °C, providing a data basis for viscosity-retarding evaluation.

#### 2.3.6. Shearing Rate Sweep Test

The zero shear viscosity test was conducted using a dynamic shear rheometer with a shear rate scanning experiment. Combined with rheological modeling and fitting analysis, the zero shear viscosity could be obtained. The shear rate scanning experiment measured the rotation speed and torque of the circular plate to obtain viscosity. By continuously applying different torques, the viscosity at different shear rates could be obtained, thus obtaining the flow curve of the asphalt sample [27]. The specific calculation procedures could be found elsewhere [28]. This method was used to evaluate the rheological properties of HVMA.

#### 2.3.7. Multiple Stress Creep Recovery (MSCR) Analysis

The multiple stress creep recovery (MSCR) test using a dynamic shear rheometer (DSR) was conducted to evaluate the elastic recovery of HVMA at temperatures ranging from 58 °C to 82 °C, under creep stresses of 0.1 kPa and 3.2 kPa with intervals of 6 °C. The MSCR test involved applying a 1 s creep load followed by a 9 s recovery period for each cycle. The strain recovery and nonrecoverable creep compliance were computed in accordance with AASHTO 70-1 [29]. In this study, the recovery percentage at 3.2 kPa ( $R_{3.2}$ ) and the non-recoverable creep compliance at 3.2 kPa ( $J_{3.2}$ ) were used as indicators, and each sample was tested twice with duplicates, with the average value taken. The specific calculation procedures could be found elsewhere [30].

#### 2.3.8. Liner Amplitude Sweep (LAS) Test

The LAS test was utilized to evaluate the intermediate-temperature performance based on AASHTO TP101 [31]. The standard loading procedure for the LAS test involved applying controlled strain loadings, with the sinusoidal load amplitude increasing linearly

from 0.1% to 30% within 5 min at a frequency of 10 Hz in, and a test temperature of 20 °C. In this study, the LAS test conducted over a duration of 5 min was referred to as LAS-5. This method was used to measure the fatigue life of HVMA.

### 2.3.9. Frequency Sweep (FS) Test

In this study, FS tests were conducted at temperatures of 85 °C, 65 °C, 45 °C, 25 °C, and 5 °C to provide sufficient data basis for constructing rheological master curves. Sweeping from 5 °C to 35 °C used an 8 mm rotor, while scanning from 40 °C to 100 °C used a 25 mm rotor. The frequency range of the scanning was 0.1 to 100 Hz. The strain level employed was 1%. More detailed information could be found elsewhere in references. It should be noted that each asphalt binder was tested twice, and the average values were used in this study [32,33]. This method was used to evaluate the complex rheological properties of HVMA.

### 2.4. Evaluation Method

This study employed an evaluation method to assess the effectiveness of viscosity-retarding by comparing the area enclosed by the viscosity–temperature curve and the coordinate axis (as shown in Figure 2). The figure below illustrates the ideal viscosity–temperature curve for a warm-mixing-based viscosity-retarding asphalt (WM-VRA). It could be observed that the viscosity–temperature curve of the WM-VRA intersected with that of a typical HVMA. Within the lower temperature range of 50–100 °C, the viscosity of the WM-VRA was higher. If the area  $S_1^*$  enclosed by the viscosity–temperature curve of the WM-VRA and the coordinate axis was larger than the area  $S_1$  enclosed by the viscosity–temperature curve of the common HVMA and the coordinate axis, then it indicated that the WM-VRA demonstrated superior performance in viscosity-retarding:

$$S_D = S_1 - S_1^* \quad (1)$$

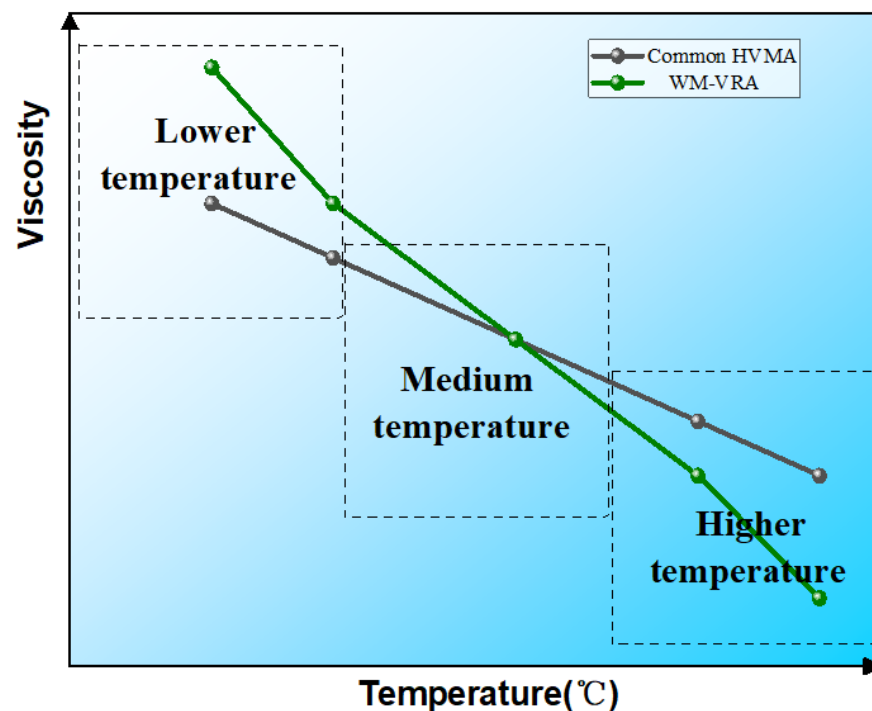


**Figure 2.** Mechanism diagram of viscosity-retarding effect.

When  $S_D$  was less than 1, HVMA was considered to exhibit a lower-temperature viscosity increase effect. A smaller  $S_D$  value indicated that the lower-temperature viscosity

of the WM-VRA was higher compared to the original sample, suggesting a better lower-temperature viscosity increase effect.

In the higher temperature range (155–200 °C), the viscosity of the HVMA was lower, and the area  $S_2^*$  enclosed by its viscosity–temperature curve and the coordinate axis was smaller than the area  $S_2$  enclosed by the viscosity–temperature curve of common HVMA.

$$S_G = S_2 - S_2^* \quad (2)$$

When  $S_G$  was greater than 1, it was considered that HVMA exhibited a higher-temperature viscosity-retarding effect. As the  $S_G$  value increases, the high-temperature viscosity of HVMA decreased compared to the original sample, suggesting a more pronounced improvement in higher-temperature viscosity reduction.

When both conditions were met simultaneously (i.e.,  $S_D < 1$  and  $S_G > 1$ ), HVMA was considered to have viscosity-retarding properties, and its viscosity-retarding effect was evaluated using a formula. As the  $S_V$  increased, the viscosity-retarding effect of HVMA improved:

$$S_V = S_G - S_D \quad (3)$$

### 2.5. Test Process

The experimental procedure framework is showed in Figure 3. Firstly, through indoor fume suppression assessment and odor level evaluation, optimal fume suppressants and their respective dosages were determined. Subsequently, various types and dosages of VRAs were added to the fume-suppressed modified asphalt. The HVMA viscosity–temperature relationship was determined through the utilization of the Brookfield rotational viscometer (RV) and temperature sweeping experiments, and the effectiveness of viscosity-retarding was evaluated using the area method. Furthermore, the internal network structure of the HVMA was examined using fluorescence microscopy, and the rheological properties of the HVMA were assessed using a dynamic shear rheometer (DSR).

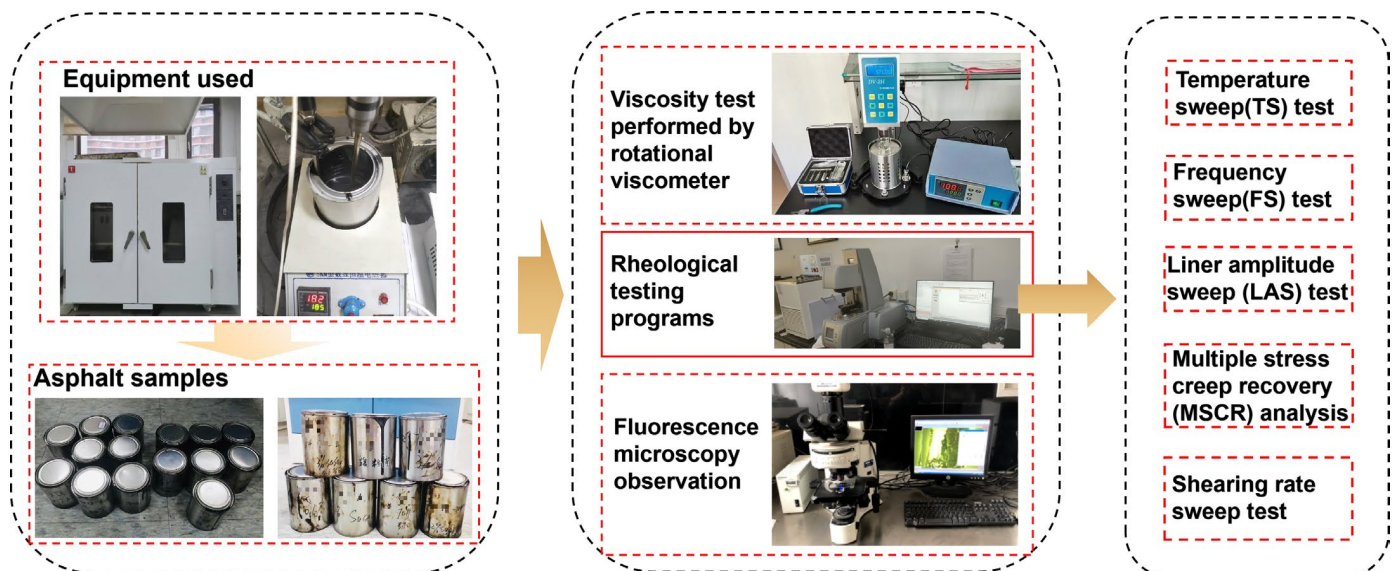


**Figure 3.** The framework of the experimental procedure.

The modification process of asphalt binder lasted for a period of two weeks, during which, potential thermal and oxidative aging could occur. In order to prevent these aging issues, it was ensured that all test quantities for each tank of HVMA samples were poured in one attempt. This approach was adopted to avoid any thermal aging that could be caused by subjecting the binder to multiple heating cycles. Simultaneously, after the pouring and cooling process, each sample was individually wrapped with silicone oil

paper. This precaution was taken to prevent any oxidation and aging problems that may arise during storage.

### 3. Results and Discussion

#### 3.1. Morphological Analysis

The FM images in Figure 4 depict the morphological features of HVMA modified with varying types and concentrations of viscosity-retarding agents (VRAs) at a magnification of 100×. In Figure 4a,b, the polymer phase is uniformly dispersed within the asphalt phase. The addition of Evotherm3G, in comparison to the control group, enhanced the network structure of high-viscosity modified asphalt (HVMA). With an increasing concentration of Evotherm3G, the network structure became more pronounced. On the other hand, in Figure 4c,d, the addition of Sasobit and fume suppressants did not impact the network structure of SBS in the asphalt, and both Sasobit and fume suppressant particles were evenly disseminated within the asphalt phase. Turning to Figure 4e,f, the presence of both Sasobit and Evotherm3G led to a complex structure in HVMA, where the network structure was less apparent compared to HVMA with a single component added. Nevertheless, a continuous spatial network structure still existed. This observation might arise from a series of unknown reactions that occur when both additives are simultaneously introduced, potentially influencing the subsequent generation of a crosslinked network. Further comprehensive investigation is required to unravel the underlying mechanisms.

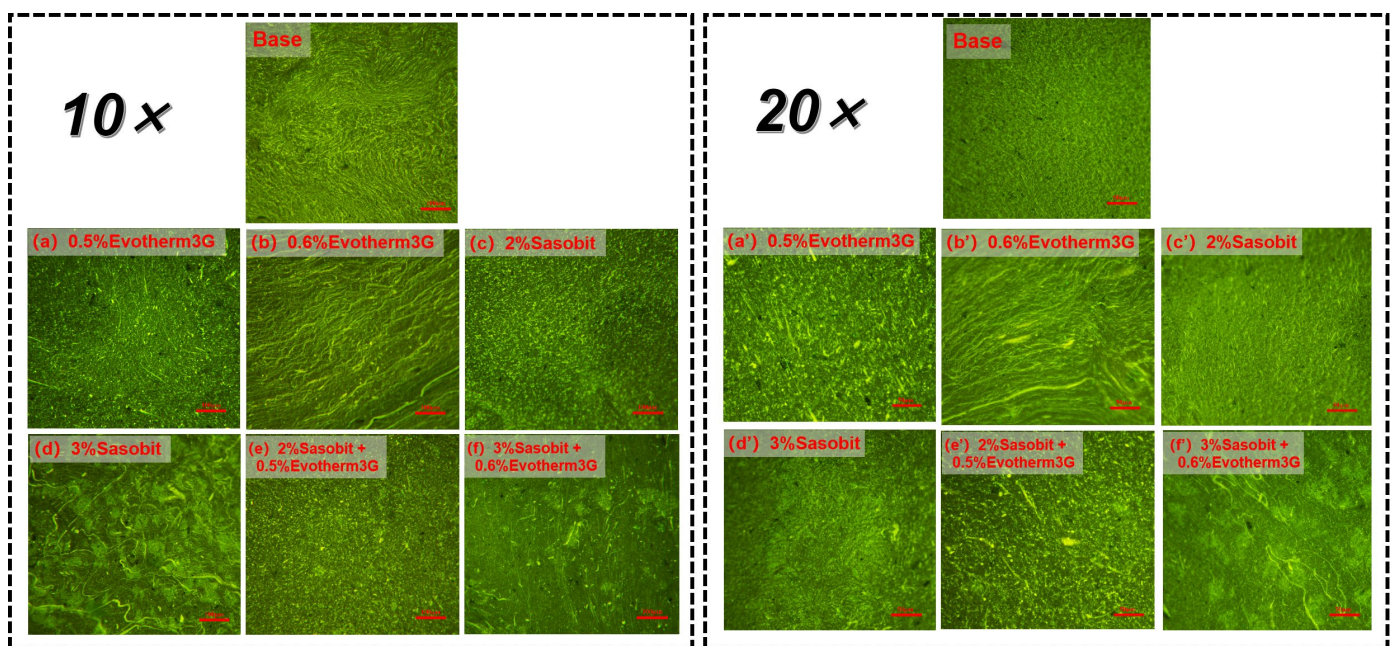


**Figure 4.** Fluorescence micrograph of different HVMA.

#### 3.2. Fume-Suppressing Effect Evaluation

Figure 5 shows the fume release and odor levels of different HVMA based on indoor fume assessment and odor level assessment described in Sections 2.3.2 and 2.3.3. According to Figure 5, it is evident that the fume suppression effect and odor level of HVMA using different types of fume suppressants (activated carbon; chemical reaction fume suppressants) were usually better than unmodified asphalt without fume suppressants. Compared with the use of chemical reaction fume suppressants, the addition of activated carbon had a slightly better fume suppression effect, but had a higher odor level. The odor level of HVMA chemical reaction fume suppressants with 15% DRP added was one level higher than that of activated carbon. This difference might be attributed to the composition of chemical reaction inhibitors—zinc castor oleate and vulcanization accelerators. The zinc oxide presented in the vulcanization promoter forms a zinc salt with the help of stearic acid.

This zinc salt was soluble in asphalt, improving the vulcanization efficiency of HVMA, thereby enhancing its high-temperature stability, and indirectly reducing the emission of foul gases such as  $H_2S$  and  $SO_2$  during the vulcanization process of the stabilizer. In addition, zinc castor oil effectively eliminated odors through chemical reactions between internal active zinc atoms and the generated sulfur and nitrogen substances. Activated carbon exhibited significant adsorption capacity for asphalt fume through its inherent adsorption principle, visually reducing fume emissions.

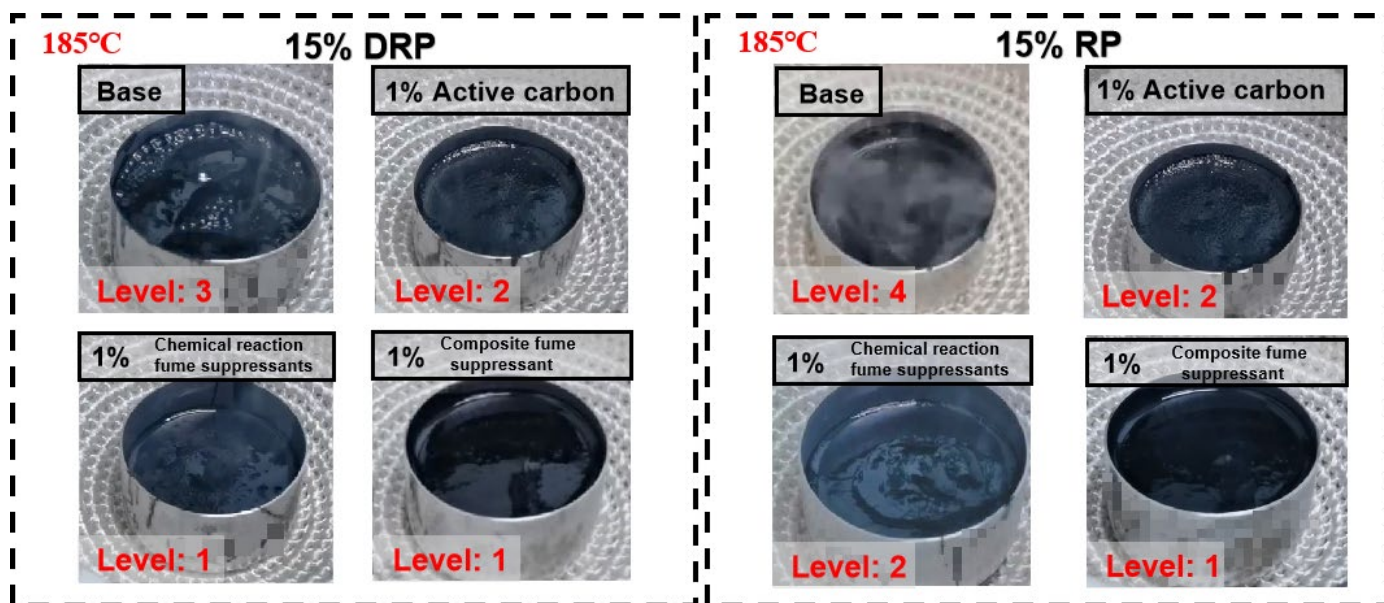


Figure 5. Emission of HVMA fume gas under different fume suppressants.

The emission of fumes from HVMA was significantly improved when composite odor-removing agents were added, compared to modified asphalt with single-component additives. And the odor levels were all level 1, which is superior to the odor level of adding chemical reaction fume suppressants and activated carbon separately. This suggested a synergistic effect between activated carbon and chemical reaction fume suppressant. Therefore, the 1% composite fume suppressant could be considered the optimal choice in this study. Additionally, the fume emission and odor level from high-viscosity modified asphalt (HVMA) with the addition of desulfurization rubber powder (DRP) were lower than ordinary rubber-powder HVMA. This indicated that 15% DRP could be deemed as an effective asphalt additive in this study. This was because the desulfurized rubber powder was a byproduct of ordinary rubber powder that underwent a desulfurization process, resulting in a significant reduction in sulfur content compared to regular rubber powder. As a result, it helped to prevent the generation of foul gases such as hydrogen sulfide, which arose from the breaking of sulfur bonds in rubber.

### 3.3. Energy-Saving Effect Evaluation

#### 3.3.1. Rotational Viscosity Test Analysis

As depicted in Figure 6a, the viscosity of all seven types of HVMA showed a decreasing trend as the temperature increases. HVMA conditioned with VRAs exhibited a more pronounced decrease in viscosity compared to common HVMA. Among these, the most significant viscosity reduction was achieved when adding 2% Sasobit, 2% Sasobit, and 0.6% Evotherrm3G + 3% Sasobit to the asphalt separately. This could be attributed to the fact that, at elevated temperatures, the solid particles of Sasobit dissolved completely in the asphalt, leading to the formation of a liquid structural wax film, ultimately resulting in a reduction in asphalt viscosity [34].

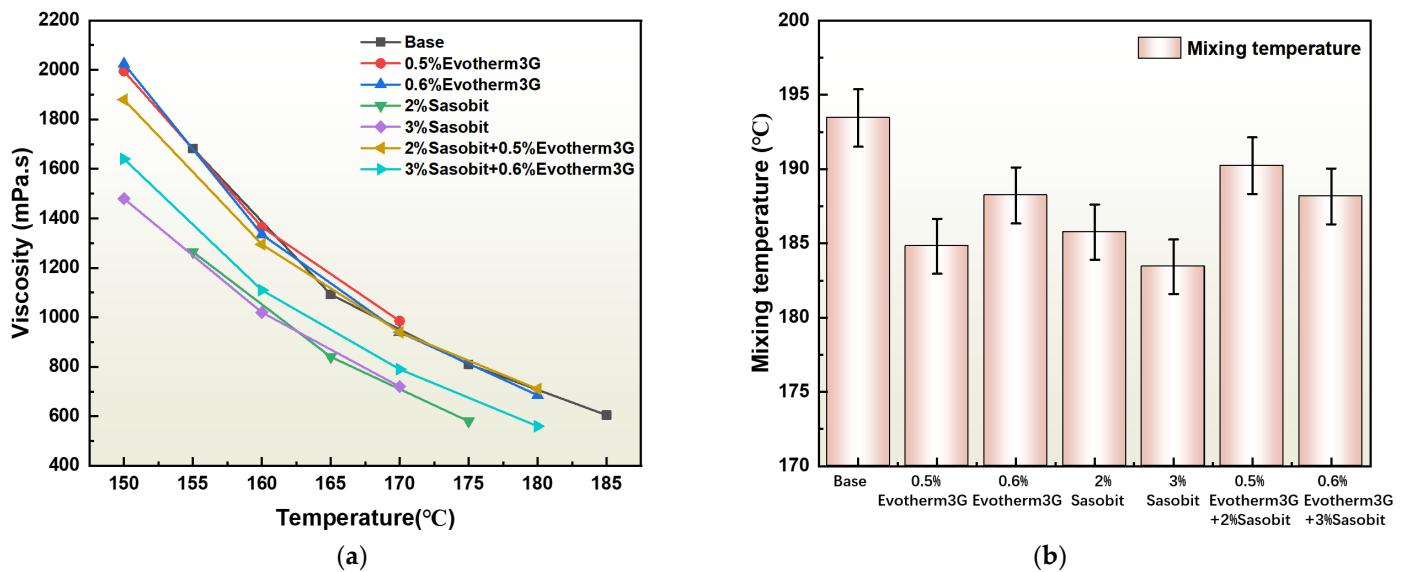


**Figure 6.** The viscosity temperature curve (a) and mixing temperature (b) of HVMA under different VRAs.

Compared to regular HVMA, the addition of Evotherm3G led to a reduction in viscosity, although it still remained higher than that of Sasobit additives. The mixing temperature of different HVMA formulations could be determined by analyzing the viscosity–temperature curve, as depicted in Figure 6b. Notably, the mixing temperature of regular HVMA was the highest, reaching 193 °C, while the mixing temperature of single-component VRAs asphalt was the lowest. The rotational viscosity of HVMA after incorporating Evotherm3G did not differ significantly from that of regular HVMA, but the mixing temperature was lower. This suggested that although the initial addition of Evotherm3G might result in an increase in HVMA viscosity, its viscosity decreased more rapidly as the temperature rises. In the end, there was no substantial difference in the final mixing temperature when compared to HVMA supplemented solely with Sasobit as an additive. Furthermore, when compared to single-component additives, the mixing temperature of the two HVMA groups with composite VRAs was slightly higher. However, the HVMA formulation with 0.6% Evotherm3G + 3% Sasobit did not significantly differ from the HVMA formulation with 0.6% Evotherm3G alone. Hence, this specific combination could be deemed as an appropriate dosage for achieving the desired viscosity reduction in this eco-friendly HVMA formulation.

### 3.3.2. Evaluation of the Viscosity-Retarding Effect

Based on the previously obtained viscosity–temperature curve, a polynomial was employed to accurately fit the data. Moreover, temperature scanning experiments were conducted to measure the complex viscosity of different high-viscosity asphalt samples within the temperature range of 30 °C to 100 °C (as depicted in Figure 7a). The viscosity-retarding performance of HVMA was evaluated using the on the integral area method (as shown in Table 1). The areas enclosed by each HVMA sample and the coordinate axes conditions were separately calculated under higher temperatures and lower temperatures. The outcomes of the integral area calculations for seven groups of HVMA samples are presented in Figure 7. The results were accurate to one decimal place with Scientific notation (Table 2).

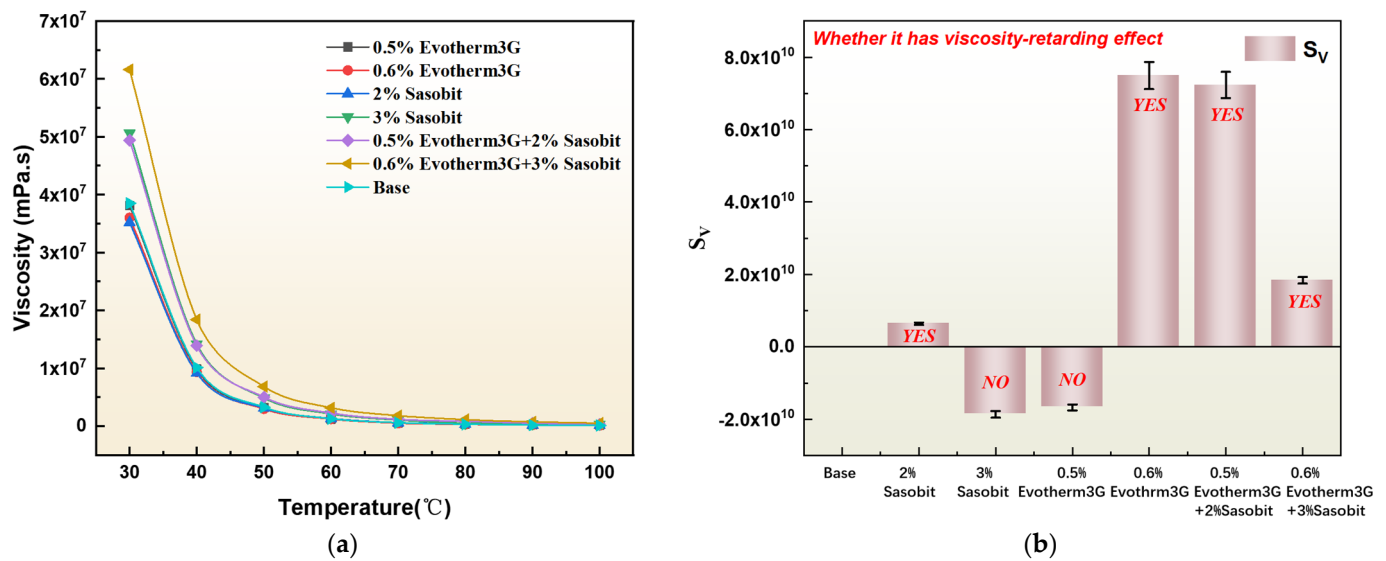


Figure 7. The low temperature complex viscosity curve (a) and viscosity-retarding effect results of HVMA under different VRAs (b).

Table 2. Results of the viscosity-retarding effect.

| Additive                     | S <sub>1</sub>         | S <sub>2</sub>        | S <sub>G</sub>          | S <sub>D</sub>         | Retarding Viscosity Effect Presence (Yes/No) | S <sub>v</sub>         |
|------------------------------|------------------------|-----------------------|-------------------------|------------------------|--|------------------------|
| Base                         | 5.9 × 10 <sup>10</sup> | 4.9 × 10 <sup>4</sup> | 0                       | 0                      | --   | --                     |
| 0.5% Evotherm3G              | 4.2 × 10 <sup>10</sup> | 6.5 × 10 <sup>4</sup> | 1.7 × 10 <sup>10</sup>  | -1.6 × 10 <sup>4</sup> | No   | --                     |
| 0.6% Evotherm3G              | 1.3 × 10 <sup>11</sup> | 4.2 × 10 <sup>4</sup> | -7.5 × 10 <sup>10</sup> | 7.0 × 10 <sup>3</sup>  | Yes  | 7.5 × 10 <sup>10</sup> |
| 2% Sasobit                   | 6.5 × 10 <sup>10</sup> | 3.9 × 10 <sup>4</sup> | -6.4 × 10 <sup>9</sup>  | 1.0 × 10 <sup>4</sup>  | Yes  | 6.4 × 10 <sup>9</sup>  |
| 3% Sasobit                   | 4.0 × 10 <sup>10</sup> | 4.2 × 10 <sup>4</sup> | 1.9 × 10 <sup>10</sup>  | 6.6 × 10 <sup>3</sup>  | No   | --                     |
| 2% Sasobit + 0.5% Evotherm3G | 1.3 × 10 <sup>11</sup> | 4.2 × 10 <sup>4</sup> | -7.2 × 10 <sup>10</sup> | 7.1 × 10 <sup>3</sup>  | Yes  | 7.2 × 10 <sup>10</sup> |
| 3% Sasobit + 0.6% Evotherm3G | 7.7 × 10 <sup>10</sup> | 2.4 × 10 <sup>4</sup> | -1.8 × 10 <sup>10</sup> | 2.5 × 10 <sup>4</sup>  | Yes  | 1.8 × 10 <sup>10</sup> |

According to the data in Table 1, it was evident that the S<sub>G</sub> value of HVMA containing 0.5% Evotherm3G and 3% Sasobit was greater than 0, indicating that these two HVMA did not achieve any low-temperature viscosity increasing effect. It could be seen that the addition of single-component Sasobit and Evotherm3G not only reduced high-temperature viscosity, but also led to a decrease in low-temperature viscosity. This was because when Sasobit and Evotherm3G were added separately, the long-chain hydrocarbons in Sasobit melted and formed an organic wax film inside HVMA, while Evotherm3G generated a structural water film inside the asphalt during the addition process, thereby reducing friction between asphalt molecules and further reducing the viscosity of the mixture [34].

The composition of HVMA with 0.6% Evotherm3G, 2% Sasobit, 0.5% Evotherm3G + 2% Sasobit, and 0.6% Evotherm3G + 3% Sasobit satisfied the criteria of S<sub>D</sub> values less than 0 and S<sub>G</sub> values greater than 0. By comparing the S<sub>v</sub> values of these three methods, the ranking of the viscous effects could be established as follows: 0.6% Evotherm3G > 0.5% Evotherm3G + 2% Sasobit > 0.6% Evotherm3G + 3% Sasobit > 2% Sasobit (as indicated in Figure 7). This analysis revealed that Evotherm3G played a primary role in promoting slow adhesion in HVMA, with 2% Sasobit being the next most effective additive.

### 3.4. Rheological Performance Characterization

#### 3.4.1. Shearing Rate Sweep Test Analysis

The flow curve of the eco-friendly asphalt is shown in Figure 8. When the shear stress surpassed the yield stress, the asphalt underwent gradual orientation, extension, deformation, and dispersion in the direction of flow, which exhibited a Newtonian flow state known as the Newtonian flow region. Within this region, the viscosity approaches a constant value, which was referred to as zero shear viscosity (ZSV). A higher ZSV for asphalt materials signified a greater resistance to long-term deformation under load, improved asphalt film on aggregate surfaces, enhanced adhesion, increased water stability, and heightened fatigue resistance.

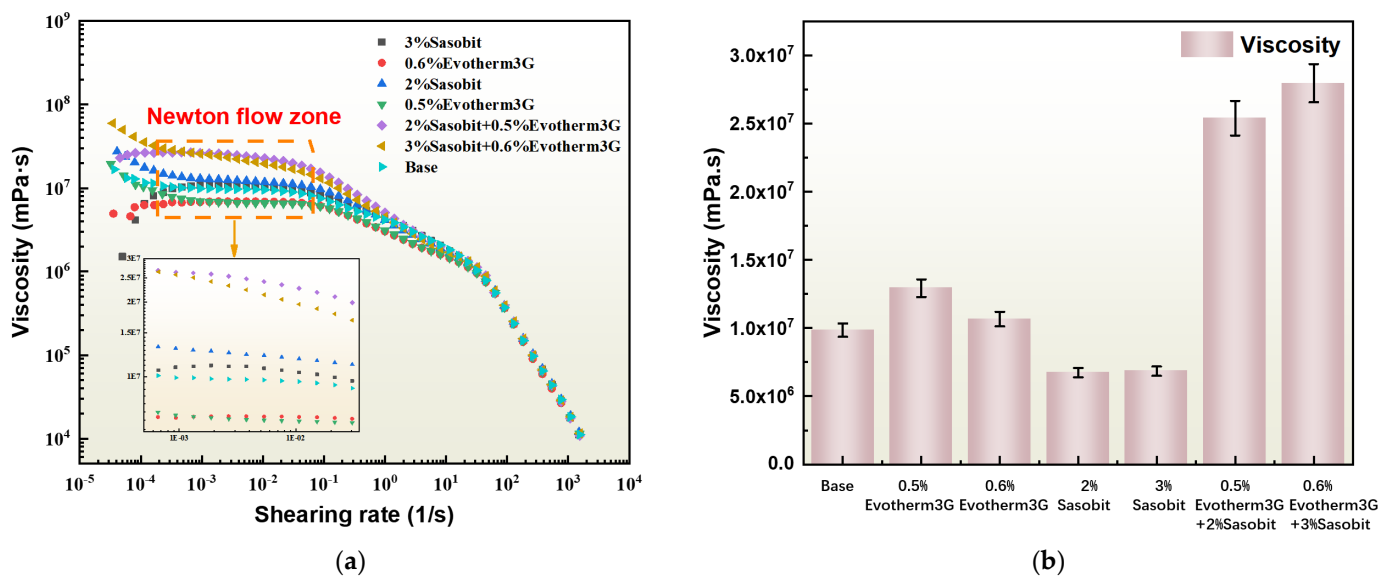


**Figure 8.** Scatter plots (a) and bar plots (b) of zero shear viscosity of HVMA under different VRAs.

Figure 8 depicts that the ZSV of the modified asphalt, containing varying amounts of single-component Sasobit, surpassed that of the blank control group. This observation suggested that the incorporation of Sasobit enhanced the long-term load deformation resistance of the modified asphalt to some extent. It is worth noting that compared to HVMA with 2% Sasobit added, HVMA with 3% Sasobit added had a slightly lower zero shear viscosity. This could be attributed to the organic wax-based nature of Sasobit, which upon increasing dosage, formed an organic wax film within the asphalt. Consequently, this film acted as a lubricant, thereby slightly reducing the viscosity of the HVMA [34]. Furthermore, the ZSV of the HVMA, incorporating single-component Evotharm3G, was lower than that of the blank control group. This discrepancy might be attributed to the formation of a structural water film due to the presence of the surfactant, which subsequently led to a decrease in asphalt viscosity [35]. While the decrease in ZSV resulted in a reduced deformation resistance of the HVMA after adding Evotharm3G, it also implied that the HVMA could more easily attain the required viscosity for mixing, effectively reducing the mixing temperature. The difference in ZSV between high and low contents of Evotharm3G was not significant, indicating that the viscosity decrease in the HVMA with increasing content of Evotharm3G was not pronounced, and it still maintained the deformation resistance at low content.

The ZSV of the composite VRAs Sasobit/Evotharm3G at high and low contents was significantly higher compared to the addition of either of the two single-component additives or the blank control group. This indicated that the combination of these two additives could significantly enhance the deformation resistance of the HVMA by possibly operating through different mechanisms. These distinct mechanisms of action between Sasobit and Evotharm3G resulted in varying effects of the two additives on the viscosity of

the mixture, consequently leading to an increase in solute concentration within the mixture system [21,24]. As a result, the ZSV was elevated. Although the ZSV of the high-content composite additive was slightly lower than that of the low-content additive, the overall difference between the two was minimal.

### 3.4.2. Multiple Stress Creep Recovery (MSCR) Analysis

The Multiple Stress Creep and Recovery (MSCR) test was widely considered as the preferred method for characterizing the high-temperature performance of asphalt binders. This test results accurately reflected the elastic recovery properties of HVMA, as shown in Figure 9. Specifically, the parameter  $R_{3,2}$  provided a direct reflection of the binder's elastic recovery, allowing for the evaluation of its elastic response and dependency. Furthermore,  $J_{3,2}$  represented the non-recoverable creep compliance of the binder, serving as an indicator of the asphalt binder's resistance to permanent deformation under repeated loading at high temperatures. In this study, the recovery rates  $R_{0,1}$ ,  $R_{3,2}$ , and non-recoverable creep compliance  $J_{nr0,1}$ ,  $J_{nr3,2}$  of various HVMA types were plotted at stress levels of 1.0 kPa and 3.2 kPa, while considering a range of temperatures, respectively.

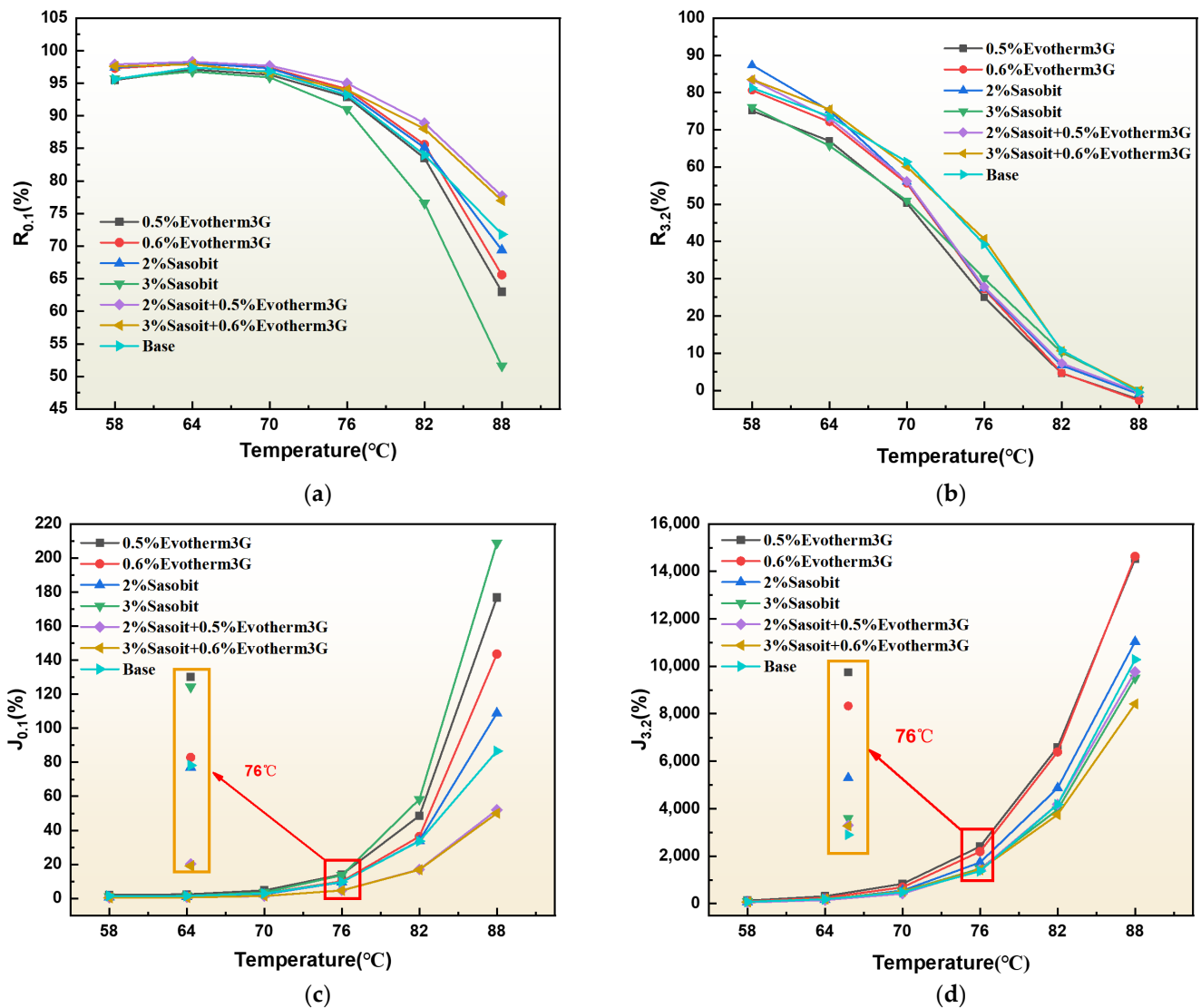


Figure 9. The  $R_{0,1}$  (a),  $R_{3,2}$  (b), and  $J_{0,1}$  (c),  $J_{3,2}$  (d) of HVMA under different VRAs.

Figure 9a illustrates the relationship between  $R_{0,1}$  and experimental temperature for seven asphalt samples that were subjected to a stress of 0.1 kPa. The horizontal axis

represents the experimental temperature, while the vertical axis represents the elastic recovery rate. Initially, the creep recovery rate of the blank control group decreased slightly as the temperature rose. However, when the temperature reached around 75 °C, the creep recovery rate sharply decreased. The  $R_{0.1}$  of the other six modified HVMA samples also decreased with increasing temperature. Among them, the sample with only one type of VRA showed a much larger decrease compared to the blank control group, especially the sample with 3% Sasobit, which exhibited the greatest decrease. This decrease could be attributed to the degradation of polymers in HVMA at high temperatures, leading to a significant decrease in creep recovery rate. On the other hand, samples with a combination of two rejuvenators showed higher creep recovery rates than the blank control group, and the rate of decrease was slower compared to the blank control group. This was because the addition of both can improve the cohesion between asphalt molecules, forming a more compact structure, thereby improving the elastic recovery performance of asphalt.

Figure 9b depicts the relationship between the  $R_{3.2}$  and experimental temperature of seven asphalt samples under a stress of 3.2 kPa. The creep recovery rate of all seven groups of samples continuously decreased with the increase in temperature. In the initial stages, the decline rate of HVMA was relatively slow as the temperature rises. When the temperature reached around 75 °C, the creep recovery rate sharply decreased. Except for the HVMA with 0.5% Sasobit and 3% Sasobit added, the  $R_{3.2}$  of the six groups of samples with VRA was not significantly different from the blank control group. Among them, the  $R_{3.2}$  of HVMA after 0.6% Evotherm3G + 3% Sasobit was slightly higher than that of ordinary HVMA. This indicated that the elastic recovery performance of HVMA had been enhanced to a certain extent after the addition of composite VRA. Figure 9c illustrates the relationship between  $J_{nr0.1}$  and experimental temperature for seven asphalt samples subjected to a stress of 0.1 kPa. Prior to reaching a temperature of 76 °C, the increase in  $J_{nr0.1}$  was relatively gradual compared to the control group. The differences in  $J_{nr0.1}$  among the seven groups of samples were not statistically significant, suggesting that HVMA demonstrated similar resistance to rutting within this temperature range. However, after the temperature surpassed 76 °C,  $J_{nr0.1}$  displayed a sudden increase, and the samples with a single VRA exhibited higher  $J_{nr0.1}$  values compared to those with common HVMA. This observed variance could be attributed to the degradation of polymers in HVMA at high temperatures, which correlated with the trend observed in  $R_{0.1}$ . It is noteworthy that the introduction of combination VRAs demonstrated robust resistance to rutting. Specifically, under high-temperature conditions, the upward trend of  $J_{nr0.1}$  was noticeably slower and considerably lower compared to common HVMA. These findings indicated that HVMA with composite VRA had excellent resistance to rutting under a stress of 0.1 kPa in high-temperature conditions.

Figure 9d depicts the relationship between  $J_{nr3.2}$  and experimental temperature for seven asphalt samples subjected to a stress of 3.2 kPa. Prior to reaching a temperature of 76 °C, the  $J_{nr3.2}$  values of the seven HVMA were found to be higher than that of common HVMA. This suggested that HVMA exhibited weaker resistance to rutting than common HVMA within the mid-temperature range, although the difference was not statistically significant. However, as the temperature exceeded 76 °C, the  $J_{nr3.2}$  values of the three groups with 3% Sasobit, 0.5% Evotherm3G + 2% Sasobit, and 0.6% Evotherm3G + 3% Sasobit VRAs decreased compared to that of common HVMA. Among these, the reduction was most pronounced for the 0.6% Evotherm3G + 3% Sasobit group. These findings indicated that under a stress of 3.2 kPa, high-dosage combination VRAs exhibited excellent resistance to rutting in high-temperature conditions for HVMA.

### 3.4.3. Analysis of Fatigue Life Prediction from LAS Test

Figure 10 illustrates the fatigue life values of different HVMA under different strain conditions (2.5%, 5%). For a strain condition of 2.5%, except for 0.6% Evotherm3G + 3% Sasobit, the fatigue life of HVMA with other additives exhibited higher values compared to ordinary HVMA. It is worth noting that HVMA with the addition of 2% Sasobit,

3% Sasobit, and 0.5% Evotherm3G + 2% Sasobit, respectively, had a higher fatigue life, with an  $N_f$  value exceeding 40,000. The reason for this notable improvement could be attributed to the addition of Sasobit, which increased the zero shear viscosity of HVMA. This, in turn, ensured that the asphalt maintains high stability, effectively resisting road reactions and preventing oxidation damage even under high temperature conditions. As a result, the durability and fatigue life of the asphalt were substantially improved. While an increase in the dosage of single-component Sasobit marginally improved the fatigue life of HVMA, the enhancement was not particularly significant. Remarkably, the  $N_f$  value of 0.5% Evotherm3G + 2% Sasobit reached as high as 45,300, which stood as the highest fatigue life value among the seven groups of HVMA.

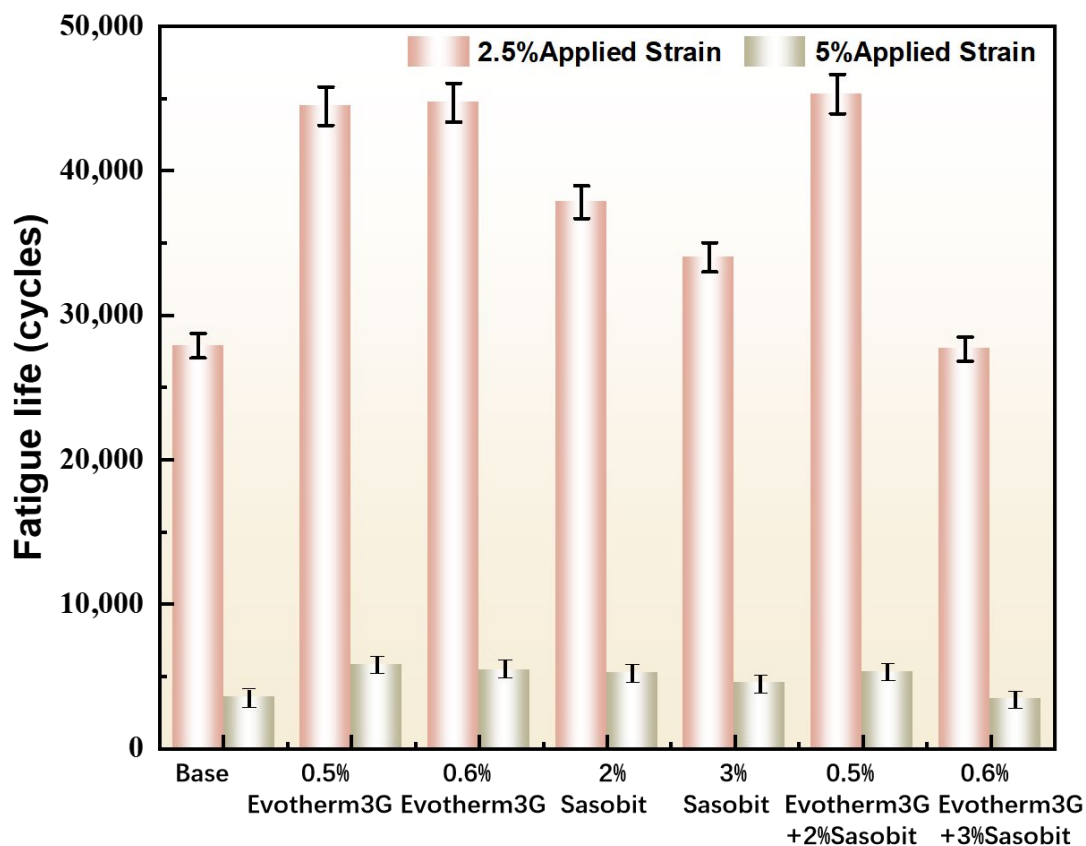


Figure 10. Fatigue life for tested HVMA.

The fatigue life of HVMA with the addition of the VRA Evotherm3G was slightly lower compared to Sasobit, but still higher than that of common HVMA. As the dosage of Evotherm3G increased, the fatigue life began to decrease slightly. Among them, the fatigue life of HVMA after adding 0.6% Evotherm3G + 3% Sasobit was 27,658, which had the lowest fatigue life among the seven groups of HVMA, but still met the requirements for road performance. It could be inferred that increasing the dosage of Sasobit further enhanced the fatigue life of the HVMA, while increasing the dosage of Evotherm3G slightly decreased the fatigue life of the HVMA. This could be attributed to a series of unknown reactions between Evotherm3G and Sasobit, resulting in a decrease in fatigue life. However, further research is needed to provide additional evidence. Considering various performance indicators of the HVMA, adding 0.5% Evotherm3G + 2% Sasobit and 0.6% Evotherm3G + 3% Sasobit remained the optimal choice for eco-friendly HVMA in this screening process.

#### 3.4.4. Frequency Sweep Test Results

Figure 11 illustrates the relationship between the complex modulus and phase angle of different HVMA samples with varying frequencies. A comparison of the seven images

revealed that, during the high-temperature stage at 85 °C, the complex modulus of the blended HVMA with Sasobit/Evotherm3G demonstrated a significantly higher value compared to the other five groups. Specifically, the main curve of the complex modulus for the sample containing 0.6% Evotherm3G + 3% Sasobit exhibited a particularly noticeable increase when compared to the remaining six groups. This finding suggested that the addition of both Sasobit and Evotherm3G enhanced the elasticity of HVMA, thereby improving its high-temperature performance for road applications. This improvement could be attributed to the ability of Sasobit and Evotherm3G to enhance the fluidity and plasticity of asphalt by altering its viscosity and flow characteristics, resulting in a higher deformation capacity and improved crack resistance. Consequently, the high-temperature stability of HVMA was significantly enhanced [21].

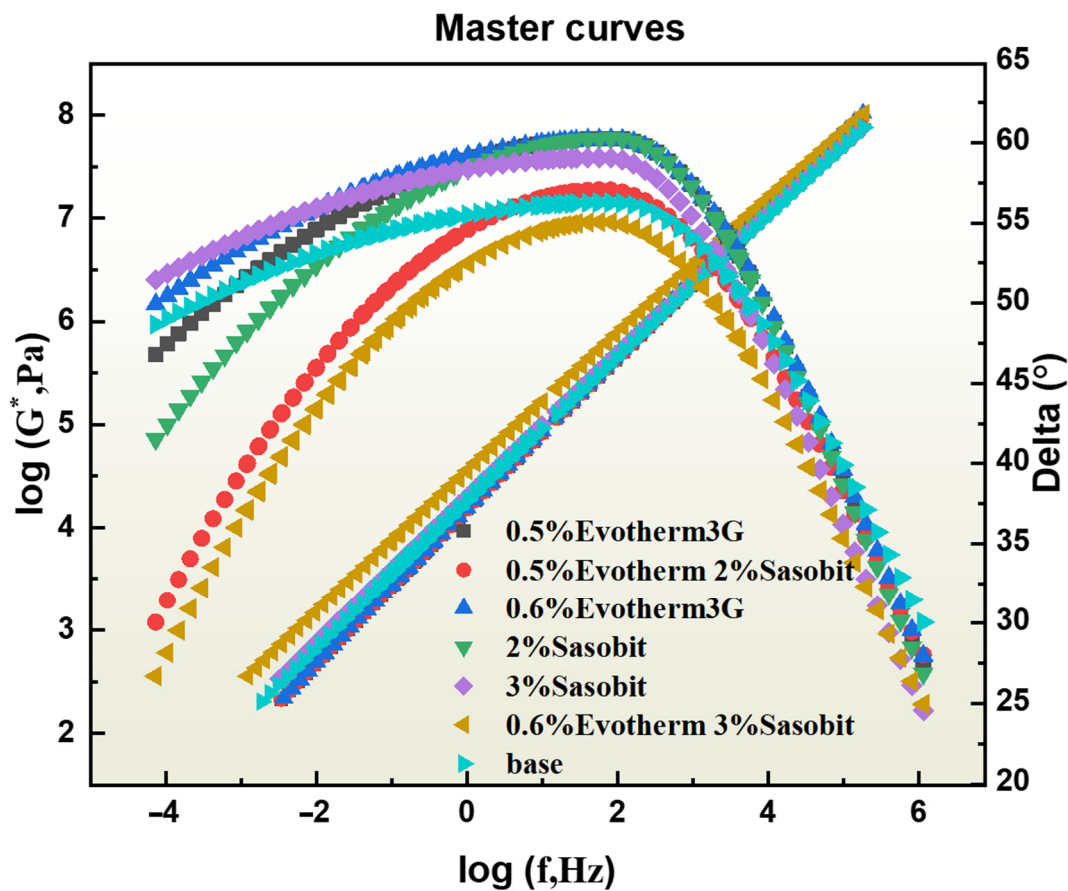


Figure 11. Moduli and phase angles of HVMA under different VRAs.

Figure 11 illustrates the relationship between the complex modulus and phase angle main curves as a function of frequency. Upon observation, it was evident that the main curves of the HVMA samples displayed an increasing trend in the complex modulus with a higher frequency. Conversely, the main curves of the phase angle initially increased and then decreased. The low-frequency region represented the high-temperature characteristics of HVMA, whereas the high-frequency region represented its low-temperature behavior. Consequently, an elevation in temperature corresponded to a decrease in the complex modulus of HVMA. When comparing the main curves of the complex modulus for various VRAs within the HVMA, it became apparent that, with the exception of the sample containing 0.6% Evotherm3G + 3% Sasobit, the differences in complex modulus in the low-frequency region were minimal; this indicated that the remaining HVMA groups exhibited similar properties to common HVMA. However, due to the limitations imposed by high frequencies (low temperatures) on the movement of asphalt molecules in HVMA, the im-

pect of VRA type and dosage on the complex modulus gradually weakened. Consequently, all the modulus curves converged to a single intersection point at high frequencies.

Upon analyzing the main curves of the phase angle, it was discerned that all seven groups of HVMA exhibited an increase followed by a subsequent decrease in the phase angle. This decrease in the high-frequency region was primarily attributed to the volatilization and transformation of light components within the asphalt. These transformations influenced the elastic response of the asphalt, ultimately leading to an enhancement in its overall elasticity. Conversely, the dominant factor affecting the phase angle was the degradation behavior of the polymer network within the HVMA. The degraded network structure was unable to provide additional elasticity to the HVMA, resulting in an increase in the phase angle. Notably, it was observed that as the dosage of the VRA increased, the polymer content within the HVMA similarly rose, thereby causing a more significant increase in the phase angle.

In high-temperature environments (specifically in the low-frequency region), the inclusion of a higher dosage of Sasobit/Evotherm3G resulted in an amplified degree of polymer crosslinking. Consequently, this led to a more noticeable decrease in the main curve of the phase angle. Conversely, the phase angle experienced minimal changes in the high-frequency region. This could be attributed to the fact that the viscoelastic properties within the high-frequency region were predominantly governed by the asphalt phase itself. Although the VRAs underwent reactions with certain functional groups within the asphalt, these reactions were relatively limited in comparison to their interactions with the polymers. As a result, the addition of the VRA did not exert a significantly impact the viscoelastic proportion of the asphalt phase.

#### 4. Conclusions and Outlook

This study evaluated the fume suppression effect and odor level of different fume suppressants on high-viscosity modified asphalt (HVMA) through indoor fume assessment firstly. Based on this, the influence of different viscosity-retarding agents (VRAs) on the mixing temperature, viscosity-retarding, and rheological properties of HVMA were investigated. The main conclusions of this research are as follows:

- (1) According to the fume-suppressing effect and odor-level evaluation results, the fume suppression effect and odor level effect of the DRP-modified HVMA was superior to that of rubber-modified HVMA when different types of fume suppressants were added. Furthermore, the ranking in terms of fume suppression effects was: composite fume agent > activated carbon > chemical reaction fume suppressant. And the odor level of adding composite fume suppressants sharply decreased to level one, far lower than the level three of ordinary base HVMA. Ultimately, it was determined that the 1% composite fume suppressants was selected as the optimal fume suppression plan.
- (2) The mixing temperatures of different HVMA were determined based on their viscosity–temperature curves. It was found that the addition of VRA could reduce the mixing temperature of HVMA to 4–10 °C. A novel method based on the integrated area of viscosity–temperature curve was proposed in this research to evaluate the viscosity-retarding effect of different VRAs. Finally, the HVMA containing with 0.6% Evotherm3G + 3% Sasobit VRAs had the optimal viscosity-retarding effect and lower mixing temperature, and was determined as the eco-friendly HVMA.
- (3) The morphological characteristics and rheological properties of various HVMA were evaluated. After Sasobit/Evotherm3G was added, the network structure of the HVMA was not as apparent as that of the HVMA with a single component added, but a continuous spatial network structure still existed. The research results of ZSV, MSCR, and LAS indicated that the selected eco-friendly HVMA exhibited better high-temperature resistance compared to common HVMA, and the fatigue life also met the performance requirements.

Overall, the focus of this study was to study an eco-friendly HVMA and propose a new evaluation method to contribute to the sustainable development of road materials.

However, this study solely illustrated the inhibitory effects of composite fume suppressants on visible fume and foul odor gases in asphalt fumes. In future research, our attention would shift toward exploring the impact of composite fume suppressants on the invisible components of asphalt fume, as well as on enhancing the evaluation method for the viscosity-retarding effect. Furthermore, we intended to broaden the scope of our investigation to encompass the fume release of asphalt mixtures during the paving process, providing technical support for the development of high-performance and eco-friendly asphalt. In addition, the material combinations selected in this study and the evaluation methods for fume suppression still needed to be further optimized.

**Author Contributions:** Methodology, G.S.; Validation, X.J.; Formal analysis, R.Z.; Investigation, W.N. and C.W.; Resources, R.Z.; Data curation, K.Q.; Writing—original draft, W.N.; Writing—review & editing, G.S. and X.J.; Visualization, K.Q.; Supervision, G.S. All authors have read and agreed to the published version of the manuscript.

**Funding:** The work described in this paper was supported by the National Natural Science Foundation of China, China (No. 52108390); Beijing Municipal Education Commission, China (No. KM202210005002); Key Laboratory of Road and Traffic Engineering of the Ministry of Education, Tongji University, China (No. K202205); Open Funding of Engineering Research Center of Ministry of Education for Traffic Pavement Materials, Chang'an University, China (No. 300102312503).

**Institutional Review Board Statement:** Not applicable.

**Informed Consent Statement:** Not applicable.

**Data Availability Statement:** Not applicable.

**Conflicts of Interest:** The authors declare no conflict of interest.

## References

1. Yang, X.; Wang, G.; Rong, H.; Meng, Y.; Liu, X.; Liu, Y.; Peng, C. Review of fume-generation mechanism, test methods, and fume suppressants of asphalt materials. *J. Clean. Prod.* **2022**, *347*, 131240. [[CrossRef](#)]
2. Cao, L.; Yang, C.; Li, A.; Wang, P.; Zhang, Y.; Dong, Z. Flue gas composition of waste rubber modified asphalt (WRMA) and effect of deodorants on hazardous constituents and WRMA. *J. Hazard. Mater.* **2021**, *403*, 123814. [[CrossRef](#)] [[PubMed](#)]
3. Tang, N.; Zhang, Z.; Dong, R.; Zhu, H.; Huang, W. Emission behavior of crumb rubber modified asphalt in the production process. *J. Clean. Prod.* **2022**, *340*, 130850. [[CrossRef](#)]
4. Li, H.; Jia, M.; Zhang, X.; Wang, Z.; Liu, Y.; Yang, J.; Yang, B.; Sun, Y.; Wang, H.; Ma, H. Laboratory investigation on fumes generated by different modified asphalt binders. *Transp. Res. Part D Transp. Environ.* **2023**, *121*, 103828. [[CrossRef](#)]
5. Cui, P.; Schito, G.; Cui, Q. VOC emissions from asphalt pavement and health risks to construction workers. *J. Clean. Prod.* **2020**, *244*, 118757. [[CrossRef](#)]
6. Xiu, M.; Wang, X.; Morawska, L.; Pass, D.; Beecroft, A.; Mueller, J.F.; Thai, P. Emissions of particulate matters, volatile organic compounds and polycyclic aromatic hydrocarbons from warm and hot asphalt mixes. *J. Clean. Prod.* **2020**, *275*, 123094. [[CrossRef](#)]
7. Clark, C.R.; Burnett, D.M.; Parker, C.M.; Arp, E.W.; Swanson, M.S.; Minsavage, G.D.; Kriech, A.J.; Osborn, L.V.; Freeman, J.J.; Barter, R.A.; et al. Asphalt fume dermal carcinogenicity potential: I. dermal carcinogenicity evaluation of asphalt (bitumen) fume condensates. *Regul. Toxicol. Pharmacol.* **2011**, *61*, 9–16. [[CrossRef](#)]
8. Bao, J.; Wang, H.; Cong, Y.; Wang, X.; Liu, S.; Wang, J.; Chen, M. Research progress of road asphalt smoke suppressant. *Contemp. Chem. Ind.* **2020**, *49*, 988–992. (In Chinese)
9. Zhang, F.; Yu, J.; Wu, S. Effect of ageing on rheological properties of storage-stable SBS/sulfur-modified asphalts. *J. Hazard. Mater.* **2010**, *182*, 507–517. [[CrossRef](#)]
10. Autelitano, F.; Garilli, E.; Pinalli, R.; Montepara, A.; Giuliani, F. The odour fingerprint of bitumen. *Road Mater. Pavement Des.* **2017**, *18*, 178–188. [[CrossRef](#)]
11. Wang, M.; Li, P.; Nian, T.; Mao, Y. An overview of studies on the hazards, component analysis and suppression of fumes in asphalt and asphalt mixtures. *Constr. Build. Mater.* **2021**, *289*, 123185. [[CrossRef](#)]
12. Mo, S.; Wang, Y.; Xiong, F.; Ai, C. Effects of asphalt source and mixing temperature on the generated asphalt fumes. *J. Hazard. Mater.* **2019**, *371*, 342–351. [[CrossRef](#)] [[PubMed](#)]
13. Yang, X.; You, Z.; Perram, D.; Hand, D.; Ahmed, Z.; Wei, W.; Luo, S. Emission analysis of recycled tire rubber Modified Asphalt in hot and warm mix conditions. *J. Hazard Mater.* **2019**, *365*, 942–951. [[CrossRef](#)] [[PubMed](#)]
14. Liang, M.; Ren, S.; Fan, W.; Wang, H.; Cui, W.; Zhao, P. Characterization of fume composition and rheological properties of asphalt with crumb rubber activated by microwave and TOR. *Constr. Build. Mater.* **2017**, *154*, 310–322. [[CrossRef](#)]

15. Wang, F.; Li, N.; Hoff, I.; Wu, S.; Li, J.; Barbieri, D.M.; Zhang, L. Characteristics of VOCs generated during production and construction of an asphalt pavement. *Transp. Res. Part D Transp. Environ.* **2020**, *87*, 102517. [[CrossRef](#)]
16. Gagol, M.; Boczkaj, G.; Haponiuk, J.; Formela, K. Investigation of volatile low molecular weight compounds formed during continuous reclaiming of ground tire rubber. *Polym. Degrad. Stabil.* **2015**, *119*, 113–120. [[CrossRef](#)]
17. Cui, P.Q.; Wu, S.P.; Xiao, Y.; Zhang, H.H. Experimental study on the reduction of fumes emissions in asphalt by different additives. *Mater. Res. Innov.* **2015**, *19*, S158–S161. [[CrossRef](#)]
18. Lv, Y.; Wu, S.; Li, N.; Cui, P.; Wang, H.; Amirkhanian, S.; Zhao, Z. Performance and VOCs emission inhibition of environmentally friendly rubber modified asphalt with UiO-66 MOFs. *J. Clean. Prod.* **2023**, *385*, 135633. [[CrossRef](#)]
19. Li, H.; Feng, Z.; Liu, H.; Ahmed, A.T.; Zhang, M.; Zhao, G.; Guo, P.; Sheng, Y. Performance and inorganic fume emission reduction of desulfurized rubber powder/styrene–butadiene–styrene composite modified asphalt and its mixture. *J. Clean. Prod.* **2022**, *364*, 132690. [[CrossRef](#)]
20. Cheraghian, G.; Falchetto, A.C.; You, Z.; Chen, S.; Kim, Y.S.; Westerhoff, J.; Moon, K.H.; Wistuba, M.P. Warm mix asphalt technology: An up to date review. *J. Clean. Prod.* **2020**, *268*, 122128. [[CrossRef](#)]
21. Jamshidi, A.; Hamzah, M.O.; You, Z. Performance of Warm Mix Asphalt containing Sasobit®: State-of-the-art. *Constr. Build. Mater.* **2013**, *38*, 530–553. [[CrossRef](#)]
22. Wan, Z.; Zheng, B.; Xie, X.; Yang, J.; Zhou, H.; Wan, R.S.; Wang, J.; Wang, J.; Luo, W.; Xue, R.; et al. Preparation method and performance test of Evotherm pre-wet treatment aluminum hydroxide type warm-mixed flame-retardant asphalt. *Constr. Build. Mater.* **2020**, *262*, 120618. [[CrossRef](#)]
23. Valdes-Vidal, G.; Calabi-Floody, A.; Sanchez-Alonso, E. Performance evaluation of warm mix asphalt involving natural zeolite and reclaimed asphalt pavement (RAP) for sustainable pavement construction. *Constr. Build. Mater.* **2018**, *174*, 576–585. [[CrossRef](#)]
24. Sukhija, M.; Saboo, N. A comprehensive review of warm mix asphalt mixtures-laboratory to field. *Constr. Build. Mater.* **2021**, *274*, 121781. [[CrossRef](#)]
25. Duan, Y. Research of the Features and Mechanism of Retardable Viscosity's Asphalt in Cold Region. Master's Thesis, Chang'an University, Xi'an, China, 2013. (In Chinese).
26. AASHTO T316; Standard Method of Test for Viscosity Determination of Asphalt Binder Using Rotational Viscometer. AASHTO: Washington, DC, USA, 2010.
27. Sun, G.; Zhu, X.; Zhang, Q.; Yan, C.; Ning, W.; Wang, T. Oxidation and polymer degradation characteristics of high viscosity modified asphalts under various aging environments. *Sci. Total Environ.* **2022**, *813*, 152601. [[CrossRef](#)] [[PubMed](#)]
28. Biro, S.; Gandhi, T.; Amirkhanian, S. Determination of zero shear viscosity of warm asphalt binders. *Constr. Build. Mater.* **2009**, *23*, 2080–2086. [[CrossRef](#)]
29. AASHTO TP 70-1; Multiple Stress Creep Recovery (MSCR) Test of Asphalt Binder Using a Dynamic Shear Rheometer (DSR). AASHTO: Washington, DC, USA, 2009.
30. Huang, W.; Tang, N. Characterizing SBS modified asphalt with sulfur using multiple stress creep recovery test. *Constr. Build. Mater.* **2015**, *93*, 514–521. [[CrossRef](#)]
31. AASHTO TP101-12; Standard Method of Test for Estimating Fatigue Tolerance of Asphalt Binders Using the Linear Amplitude Sweep. AASHTO: Washington, DC, USA, 2012.
32. Asgharzadeh, S.; Tabatabaee, N.; Naderi, K.; Partl, M. An empirical model for modified bituminous binder master curves. *Mater. Struct.* **2012**, *46*, 1459–1471. [[CrossRef](#)]
33. Asgharzadeh, S.; Tabatabaee, N.; Naderi, K.; Partl, M. Evaluation of rheological mastercurve models for bituminous binders. *Mater. Struct.* **2013**, *48*, 393–406. [[CrossRef](#)]
34. Ingrassia, L.P.; Lu, X.; Canestrari, F.; Ferrotti, G. Tribological characterization of bituminous binders with Warm Mix Asphalt additives. *Constr. Build. Mater.* **2018**, *172*, 309–318. [[CrossRef](#)]
35. Kassem, E.; Cucalon, L.G.; Masad, E.; Little, D. Effect of Warm Mix Additives on the Interfacial Bonding Characteristics of Asphalt Binders. *Int. J. Pavement. Eng.* **2018**, *19*, 1111–1124. [[CrossRef](#)]

**Disclaimer/Publisher's Note:** The statements, opinions and data contained in all publications are solely those of the individual author(s) and contributor(s) and not of MDPI and/or the editor(s). MDPI and/or the editor(s) disclaim responsibility for any injury to people or property resulting from any ideas, methods, instructions or products referred to in the content.